

TRACK FORMATION IN INDIUM PHOSPHIDE UNDER IRRADIATION BY SWIFT HEAVY IONS

A.A.Kamarou^{1,2)}, W.Wesch¹⁾, F.F.Komarov²⁾

¹⁾ Friedrich-Schiller-Universität Jena, Institut für Festkörperphysik, Max-Wien-Platz 1, D-07743 Jena, Germany, Phone: +49 3641 947330; Fax: +49 3641 947302; E-mail: wesch@pinet.uni-jena.de

²⁾ Institute of Applied Physics Problems, 7 Kurchatava St., 220064, Minsk, Belarus, Phone/Fax: +375 17 2774833; E-mail: kamarou@rfe.bsu.unibel.by

in the framework of this paper we carried out a numerical simulation of an evolution of the temperature fields that arise along the trajectories of swift heavy ions ($\{E/M\} \sim$ units of MeV/a.m.u.) in indium phosphide with regard for energy dissipation and variation of the charge state of stopping ions over the depth. Thermal spike model was used as a physical basis for calculations. The simulation results on spatial parameters of being formed tracks are in good agreement with existing experimental data. Charge state fluctuations mechanism is discussed as being responsible for discontinuous track formation.

Introduction

Ion implantation as a technological method plays very important role in the field of microelectronics. For instance, ion implantation is widely used not only for doping technical materials as well as for synthesis of new compounds, but also to change mechanical, electrical, optical and other properties of close-to-surface layers. Particularly, high-energy ion implantation is used in production of optoelectronic devices on the basis of $A_{III}B_V$ semiconductors.

Unfortunately, the processes accompanying high-energy ion implantation into semiconductors are as yet not studied properly.

This paper is devoted to a numerical simulation of track formation processes in inP for Xe^{2+} ($E = 250$ MeV, $M = 131$ a.m.u.) irradiation.

It is known that when fast multiply charged ion (in our case we have: $\{E/M\} \cong 1,9$ MeV/a.m.u.) passes through target, it loses its energy, which is mainly spent for excitation and ionization of lattice atoms (inelastic stopping). Energy losses through direct collisions with atoms (elastic stopping) become significant as compared to inelastic stopping only at the end of ion range, where ion energy decreases so, that it is not enough for efficient excitation and ionization of target atoms.

The contribution of all other processes, such as, for instance, bremsstrahlung, in energy losses is negligible along the whole range.

The model

A thermal spike model was used by the authors as a physical basis. The following system of equations for heat flows in both electronic and atomic subsystems of the crystal was used:

$$C_e(T_e) \frac{\partial T_e}{\partial t} = \frac{1}{r} \frac{\partial}{\partial r} \left[r K_e(T_e) \frac{\partial T_e}{\partial r} \right] - g(T_e - T_a) + A(r, t)$$

$$C_a(T_a) \frac{\partial T_a}{\partial t} = \frac{1}{r} \frac{\partial}{\partial r} \left[r K_a(T_a) \frac{\partial T_a}{\partial r} \right] + g(T_e - T_a)$$

where C_e and C_a are the specific heat and thermal conductivity of electrons and atoms, respectively; T_e and T_a are temperatures of electron and atomic subsystems; r is radial distance from ion trajectory; t is time; g is a coefficient related to energy transfer from electrons to the lattice; A is the energy density deposited in the target electrons.

The coefficient g can be written in the following form [1]:

$$g = \frac{\pi^2 m_e n_e v^2}{6 \tau_e (T_e) T_e},$$

where m_e is electron mass; n_e is electron concentration; v is sound velocity in the target material; τ_e is electron mean free time between two collisions.

The following expression was proposed for $A(r, t)$ [2]:

$$A(r, t) = b \frac{dE}{dz} \exp\left(-\frac{(t - t_0)^2}{2t_0^2}\right) \exp(-r/r_0),$$

where (dE/dz) is linear inelastic ion energy loss; t_0 is time required by the electrons to reach an equilibrium distribution (i.e. the flight time of average energy delta-ray electrons: $t_0 = (1-5) \times 10^{-15}$ s); r_0 is spatial width of highly excited area; b is a normalization constant chosen in the following natural way:

$$\iint A(r, t) 2\pi r dr dt = dE/dz.$$

(dE/dx) is linear inelastic energy losses over unit length of the range. The classical Bethe formula is used as an expression for the inelastic energy losses:

$$(dE/dx) = \frac{4\pi N_0 e^4 Z_{eff}^2}{m_e v^2} Z_b \text{Ln} \left[\frac{2m_e v^2}{\langle I \rangle} \right],$$

where m_e is a mass of electron, v is ion velocity, Z_{eff} is an effective projectile charge depending on its energy.

in order to calculate $\langle I \rangle$ in the case of non-monoatomic substances Bragg's rule [3] was used (chemical bonds effect was neglected):

$$S_e(A_n B_m) = n S_e(A) + m S_e(B); S_e = \frac{1}{N} (dE/dx),$$

where $A_n B_m$ is binary substance (n and m are number of atoms), S_e – electronic stopping cross-section.

Therefore we obtain:

$$Z_b \text{Ln} \left[\frac{2m_e v^2}{\langle I \rangle} \right] = Z_b^{(1)} \text{Ln} \left[\frac{2m_e v^2}{\langle I^{(1)} \rangle} \right] + Z_b^{(2)} \text{Ln} \left[\frac{2m_e v^2}{\langle I^{(2)} \rangle} \right]$$

where upper index indicates component's number. Last expression enables us to find necessary characteristics of the binary substance.

To calculate $\langle I \rangle$, mean ionization potentials of components $\langle I^{(1)} \rangle$ and $\langle I^{(2)} \rangle$ were taken from [4]. The values of N and C_v as well as δ (corresponding to temperature range near 1000 K) were taken from [5].

Mean ion charge fluctuations can be described by the formula [3]:

$$\Delta Z_{eff} = \frac{1}{2} \left\{ Z_{eff} \left[1 - \left(\frac{Z_{eff}}{Z_1} \right)^{1/k} \right] \right\}^{1/2},$$

where $k = 0.6$.

Taking into account natural requirements of limited electronic and atomic temperatures as well as their weak dependence on time at large distance from ion trajectory, we can write down the following system of equations for both initial and boundary conditions:

$$\begin{cases} T_a(r,0) = T_{init}(r) = \bar{T}_{room}, & T_e(r,0) = T_{init}(r) = \bar{T}_{room}; \\ \lim_{r \rightarrow 0} \left[r K_a(T_a) \frac{\partial T_a}{\partial r} \right] = 0, & \lim_{r \rightarrow 0} \left[r K_e(T_e) \frac{\partial T_e}{\partial r} \right] = 0; \\ T_a(R,t) = f_a(t), & T_e(R,t) = f_e(t). \end{cases}$$

The mathematical apparatus used to develop corresponding simulation code was described in details in [6].

Results and discussion

As it was mentioned earlier, we considered track formation processes in InP for Xe^+ ($E = 250$ MeV, $M = 131$ a.m.u.) irradiation to use existing experimental results [7,8].

The samples used in the experiments [7,8] were single crystalline semi-insulated (001) InP wafers. 250 MeV Xe^+ ions were implanted at room temperature with a fluence of $7 \cdot 10^{12}$ cm $^{-2}$. The structure of irradiated samples of InP was investigated by means of RBS/Channeling and TEM (transmission electron microscopy) techniques.

Let us enumerate some important results of the experiments [7,8] in brief. First, no track formation was revealed in close to the surface layer ~ 35 nm thick. Only a few black points with a size of about $2 \div 3$ nm were seen in depths $\sim (15 \div 35)$ nm. They could be both clusters of point defects and, probably, inclusions of amorphous phase. Second, the depth region between 35 nm and about $10 \mu\text{m}$ was found to contain latent tracks with a nearly circular shape of cross section; their diameter and density were estimated to be about 7 to 15 nm and $(1+2) \cdot 10^{11}$ cm $^{-2}$, respectively. Third, the depth layer from 12 to $17 \mu\text{m}$ remains crystalline (though it contains clusters of point defects) and finally, a band of heavily damaged InP occurs at a depth of 21 to $22 \mu\text{m}$ (these values correspond to mean projected ion range). The morphology of tracks also essentially depends upon depth. At low depths (up to $100 \div 300$ nm) the majority of tracks are formed of separated spherical or elongated cylindrical damaged regions. As we go deeper a gradual overlapping of the separate defects and continuous track formation were observed. The layer containing continuous tracks reaches a depth of $6 \mu\text{m}$ [7].

Thus, the experimental results themselves enable us to make obvious conclusions about complex

character of energy transfer and relaxation processes.

The main simulation results are presented in Figs. 1-3.

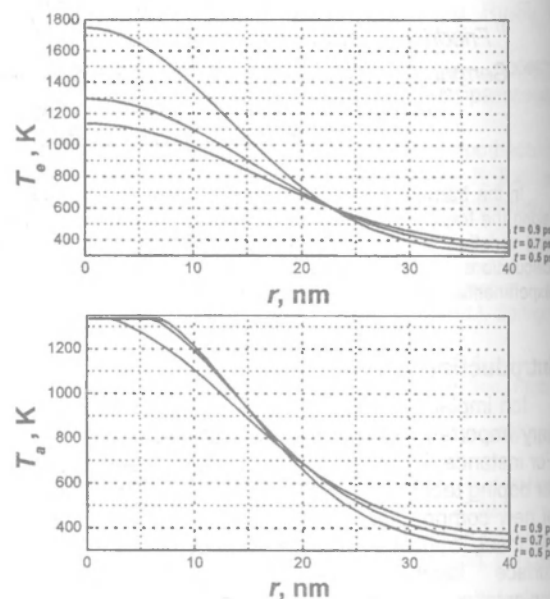


Fig. 1. Radial distribution for electronic and lattice temperature for various moments of time. A plateau corresponds to the melting point of InP (1335 K).

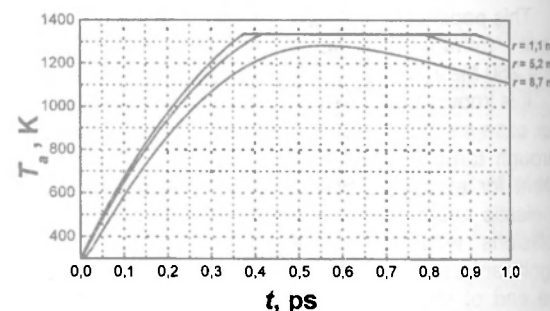


Fig. 2. An evolution of atomic temperature for different radial distances from single ion trajectory.

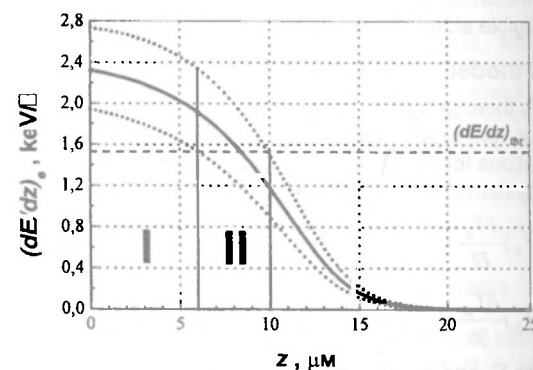


Fig. 3. Inelastic ion energy losses vs. depth. Dashed horizontal line corresponds to a threshold (for track formation) value. Dotted lines illustrate possible dynamic energy losses due to charge state fluctuations. Area I contains continuous while II – discontinuous tracks.

It is worth mentioning that all presented below results correspond to fixed value of depth $z = 1 \mu\text{m}$ (the respective value of $(dE/dz)_e$ is $2.3 \text{ keV}/\text{\AA}$).

According to the classical thermal spike model, tracks are formed in the regions along ion paths where atomic temperature reaches the melting point (1335 K for InP). In our calculations we did not take into account the latent heat of fusion, i.e. we supposed that for the latent track to be formed it is enough to heat the local area along ion path up to melting point and to supply some extra amount of energy (not necessary large). Therefore, the first figure enables us to estimate the maximum diameter of the formed latent tracks. Thus one can see that the calculated maximum track width is about $14 \mu\text{m}$. This value is in good agreement with the experimental data presented in [7,8].

With the regard for the mentioned experimental data [7,8] one can naturally suppose that there are definite "threshold" ion energy losses $(dE/dz)_{thr}$ necessary to form continuous or discontinuous tracks (so as these defects have definite length). The last figure allows to conclude that $(dE/dz)_{thr}$ is about 15 keV/nm . Discontinuous tracks can be formed due to dynamic fluctuations of number of electrons bounded to ion nucleus. Such a processes must cause fluctuations of effective charge of the ion Z_{eff} , and, therefore, must be responsible for fluctuations of $(dE/dz)_e$. Therefore, dynamical ion charge can vary as $(Z_{eff} \pm \Delta Z_{eff})$; it means that dynamical value of $(dE/dz)_e$ will fluctuate within $\pm \Delta(dE/dz)$ range. So as $(dE/dz)_e \sim Z_{eff}^2$, two-electron capture/loss processes can result in large variation of $(dE/dz)_e$ value (in our case up to 30%).

Processes including three or more bounded electrons are least probable [9] and can be neglected.

Conclusions

We carried out a numerical simulation of an evolution of the temperature fields that arise along the trajectories of swift heavy ions ($\{E/M\} \sim$ units of $\text{MeV}/\text{a.m.u.}$) in indium phosphide with regard for

energy dissipation and variation of the charge state of stopping ions over the depth. Well-known thermal spike mechanism of track formation was applied as a physical basis.

Performed numerical calculations allowed us to determine radial distributions and temporal parameters for temperature fields (thermal spikes) in both electronic and atomic subsystems of the crystal as well as to estimate "threshold" inelastic energy losses to form either continuous or discontinuous tracks in InP. Ion charge fluctuation mechanism is suggested to be responsible for formation of experimentally observed by Herre et al. [7] discontinuous tracks in InP. Obtained numerical results are in good agreement with recent experimental data [7,8].

Acknowledgements

The authors are indebted to Dr. P.I.Gaiduk for fruitful discussions. We acknowledge also financial support from from Belarusian Fund for fundamental research (grant no. F00-010).

References

1. M.Toulemonde, Ch.Dufour, Z.Wang, E.Paumier // Nucl. Instr. & Meth. B 112 (1996) 26.
2. C.Dufour, E.Paumier, M.Toulemonde // Radiat. Eff. & Defects in Solids 126 (1993) 119.
3. A.F.Burenkov, F.F.Komarov, S.A.Fedotov // Phys. Stat. Sol. (b) 169 (1992) 33.
4. Ahlen S.P., Rev. Mod. Phys. 52, No 1, (1980) P.121.
5. Series "Numerical data and functional relationships in science and technology", Springer-Verlag, Berlin-Heidelberg. "New series" (1984) Vol. 17d.
6. A.A. Kamarou, D.A. Malafei, V.S. Shcheplik // Proceedings of 2nd International Conference CFDM-98 ("Finite-difference methods: theory and applications"), Minsk, 6-9.07.1998, Vol. 2, pp. 56-62.
7. O.Herre, W.Wesch, E.Wendler, P.I.Gaiduk, F.F.Komarov, S.Klaumunzer, P.Meier // Phys. Rev. B 58 (1998) 4832.
8. W.Wesch, O.Herre, P.I.Gaiduk, E.Wendler, S.Klaumunzer, P.Meier // Nucl. Instr. & Meth. B 146 (1998) 341.
9. H.D.Betz // Rev. Mod. Phys. 44 (1972) 465.